ARMA 12-167

Calibration of FLAC3D to Simulate the Shear Resistance of Fully Grouted Rock Bolts

Tulu, I.B.
West Virginia University (WVU) Mining Engineering Department, Morgantown, WV, USA
Esterhuizen, G.S.
National Institute for Occupational Safety and Health (NIOSH), Pittsburgh, PA, USA
Heasley, K.A.
West Virginia University (WVU) Mining Engineering Department, Morgantown, WV, USA

This paper was prepared for presentation at the 46th US Rock Mechanics / Geomechanics Symposium held in Chicago, IL, USA, 24-27 June 2012.

ABSTRACT: The resistance to lateral shearing is an important yet poorly understood component of the reinforcement provided by fully grouted rock bolts. Numerical models such as the FLAC3D finite difference code can be used to investigate the effect of shear resistance on roof stability. However, calibrating a numerical model to realistically simulate the complex processes that occur at the shearing interface can be challenging. This paper outlines recent work in which a systematic procedure was developed to match numerical model results to the measured shear response of fully grouted rock bolts.

In this paper, results of the shear tests of reinforced rock joints published by Haas [1] and McHugh and Signer [2] were modeled with FLAC3D to identify and calibrate the critical parameters of the rock bolt model both in tension and in shear. In particular, the model response to changes of the bolt/joint angle and the surrounding rock type were calibrated and compared with the published tests results. It was found that the structural pile element in FLAC3D can be used to accurately represent grouted bolt shear and tensile behavior. The best approach to calibrate the FLAC3D structural pile element model was found to be: 1) select the structural element segment size less than half of the active length, 2) calibrate the shear spring cohesion and stiffness based on pull test results, and 3) calibrate the normal spring cohesion and stiffness based on shear test results. Using this method, the calibrated model results fit the test results very well.

1. INTRODUCTION

Immediately after development of an underground entry, the virgin stress field is redistributed to achieve a new stress equilibrium. As a result of this stress change, the roof beam over the entry moves downward and the vertical stress over the entry roof is relieved. When the roof beam sags, vertical and horizontal displacements take place. Fully grouted roof bolts provide reinforcement by providing a resistance to both the vertical and horizontal displacements of the roof beam. Peng [3] defined the resistance in the vertical direction as beam building and suspension, and resistance in the horizontal direction or shear restraint as “rigidity.” It is understood that the bolt’s axial resistance to vertical movement occurs at the grout/rock interface [4, 5]. However, the bolt’s shear resistance to horizontal movement is not well understood. As a result of this poor understanding of the shearing resistance of fully grouted rock bolts, the most popular roof bolt design methods only consider the axial reinforcing effect of the bolts [6].

Generally, the reinforcing effects of rock bolts are analyzed using two different testing arrangements: pull tests and direct shear tests. Pull tests quantify the reinforcing effect of the roof bolt in the axial direction, while direct shear tests quantify the shear reinforcing effect of the rock bolt.

2. BACKGROUND

Bjurström [7] performed direct shear tests on hard rock joints reinforced by fully grouted rock bolt. He discussed three reinforcement mechanisms of the rock bolt during the shearing of the bolt/joint system. First, the tangential component of the induced tensile force contributes directly to the shear resistance. Second, the normal component of the induced tensile force increases frictional resistance of the joint. Third, a “dowel effect (shear resistance to lateral movement)” is generated by the combined effect of the bolt shear strength, bending stiffness, and surrounding rock strength and stiffness.

During the shearing of the reinforced joint (regardless of the bolt type [8]), three different stages of load/displacement behavior were reported (Figure 1) [8, 9]. The first stage corresponds to linear behavior, with a

very stiff response. A rebar bolt mobilizes around 50% [9] to 75% [8] of its resistance after 1- to 5-mm shear displacement across the joint. The bolt deforms elastically in this stage. In the second stage, non-linear behavior was observed. For a fully grouted steel bolt, yielding of the steel took place in this stage with the formation of plastic hinges. McHugh and Signer [2] explained the mechanics of the formation of the hinge points on the bolt based on the investigation of the bending and axial strains on the bolt. Initially one side of the bolt extends and other side compresses near the joint surface where bending takes place. The extended side of the bolt reaches the yield strain very quickly and forms a plastic hinge point. The distance between the plastic hinges on each side of the joint are called the "active length" [10], and this active length can change depending on the strength of the surrounding rock [9]. In the third stage of load/displacement behavior, unconstrained plastic deformation of the bolt took place. According to McHugh and Signer [2], after the formation of the hinge points, the compressed side of the bolt starts to extend and yield in tension until the bolt fails due to excess tensile strain (or stress).

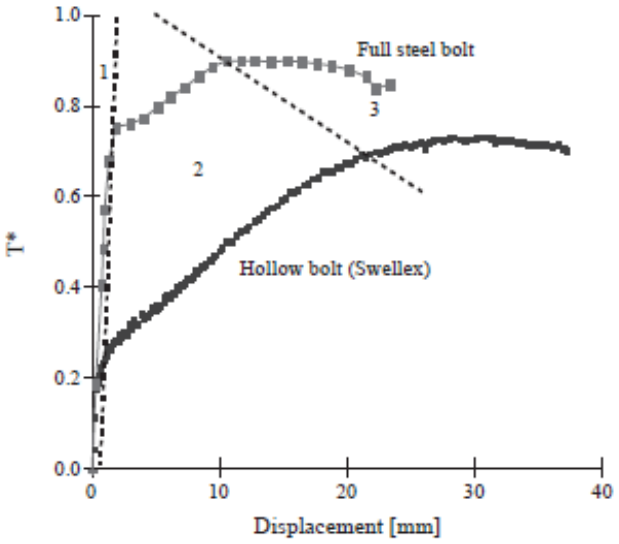

Fig. 1. Bolt contribution (T^*) vs. displacement curve [8].

Many different analytical models were developed to quantify the load/deformation behavior of a fully grouted bolt that intersects a bedding plane. Based on some experimental results, Fairhurst and Singh [11] indicated that shearing along a joint induces bending stresses in the bolt that decay very rapidly with distance into the rock. Fairhurst and Singh [11] modeled the bolt as a short beam by assuming rock to be rigid and grout to be absent over the decay length. Gerdeen et al. [12] modeled the bolt as a beam on elastic grout. Their model ignored the load transfer mechanisms around the rock. Later, many other analytical models [13, 14, 15] that assumed the bolt acted like a beam on an elastic foundation were developed. Different from the Gerdeen et al. [12] model, these models assumed that the response from the elastic foundation depended on the mechanical properties of the rock.

For the bolt, two different types of failure behavior were described in the literature. The first one is shear failure of the bolt with small deformation [7, 11, 13]. The second type of failure starts with formation of the plastic hinges by the yielding of the bolt due to a combination of axial load and bending moment (Eq. 1) [14]. Failure occurs due to the combination of shear and tensile failure (Eq. 2) [6, 14, 15], or only due to tensile failure of the bolt [13, 14]. Failure of the bolt is observed between the hinge points. This type of failure was reported by various authors [2, 8, 9].

$$\left[\frac{T_{tx}}{T_{ty}}\right]^2 + \left[\frac{M_z}{M_{pl}}\right] = 1 \qquad (1)$$

where

T_{tx} = axial load.
T_{ty} = axial yield load of the bolt.
M_z = bending moment.
M_{pl} = plastic moment.

$$\left[\frac{T_{tx}}{T_{tu}}\right]^n + \left[\frac{V}{V_u}\right]^n = 1 \qquad (2)$$

where

T_{tu} = ultimate axial load of the bolt.
V = shear load.
V_u = ultimate shear load of the bolt (50% of the ultimate axial load [5])
n = constant (depends on the bolt type [6]).

Failure behavior of the bolt depends on the strength of the surrounding rock [9]. For hard rock, the bolt is more likely to fail due to shear [7, 9] and for softer rock, tensile failure of the bolt is more likely [2, 8, 9]. The orientation of the bolt with respect to the discontinuity also affects the failure type [1, 7]. A bolt oriented perpendicular to the shear deformation is more likely to fail due to shear [7, 6]. Haas [1] performed direct shear tests on smooth joints reinforced by inclined bolts. Three orientations of the bolt were used: 45°, 90° and 135°. The 45° orientation contributed the most and 135° orientation contributed the least to the shear resistance. The effect of the pre-tensioning and post-tensioning of the grouted bars on the shear resistance was also investigated by Haas [1]. He reported that pre-tensioning or post-tensioning of the grouted bars did not show any significant effect on the shear resistance. McHugh and Signer [2] also indicated that there was not any correlation between the axial pretension load and the joint shear reinforcement, but there was a slight correlation with joint yield displacement. Haas [16] used

naturally fractured (rough) joints to investigate the effect of joint dilation on the shear resistance, and he indicated that dilation of the joints creates additional tension on the bolt.

3. NUMERICAL MODELING OF ROCK BOLTS WITH FLAC3D AND 3DEC

In the FLAC3D and 3DEC numerical codes, supports are modeled using special structural elements [17]. In these methods, the rock bolt is modeled with two noded, straight, finite elements. The interaction between the bolt and the rock zones (elements) is modeled with a spring-slider unit, with the stiffness of the springs representing the normal/shear deformation of the grout (Figure 2). The resistances of the sliders represent the normal/shear load capacity of the bolt, grout, and rock interface. The displacement of each structural element node is interpolated from the displacements of the surrounding zone grid points representing the rock. The relative displacement between the rock zone and structural element node is then calculated. The force generated at the grout/rock interface is calculated from the multiplication of the spring stiffness and relative displacement. Finally, the mobilized force at the grout/rock interface is distributed back to the rock zone grid points [17, 18].

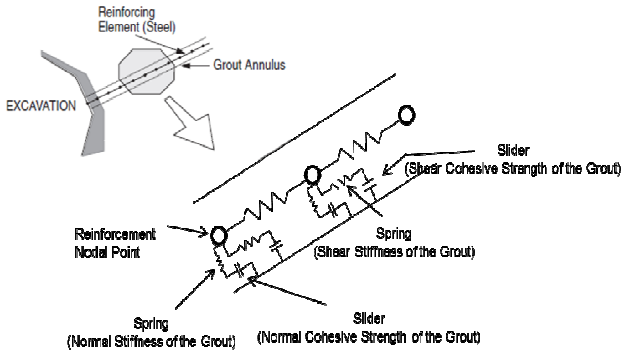

Fig. 2. Mechanical representation of fully grouted reinforcement.

FLAC3D has both cable and pile structural elements that can be used to model rock bolts. Cable elements have only one degree of freedom oriented axially and therefore can only model axial loading in the element. Pile elements have six degrees of freedom per node, and behave like a beam with normal and shear frictional interaction between the grid and pile elements (Figure 2) [17]. In FLAC3D, pile elements seem most suitable for simulating the reinforcing mechanisms of fully grouted rock bolts.

Two types of reinforcement models are provided in 3DEC (or UDEC): local and global reinforcement models [19]. The local reinforcement model considers only the local effect of reinforcement where it passes through existing discontinuities. The global reinforcement models are structural elements identical to the cable and pile elements used in FLAC3D. Therefore, the only difference between the FLAC3D and 3DEC rock bolt modeling approaches is the local reinforcement model that is solely available in 3DEC.

The local reinforcement model in 3DEC (or UDEC) assumes that, during shear displacement along a discontinuity, the reinforcement deforms as shown in Figure 3. Lorig [10] indicated that experimental results and theoretical investigations showed that shearing along a discontinuity induces bending stresses in the reinforcement that decay very rapidly with distance from the joint. Shear tests of reinforced discontinuities performed by other researchers support this assumption [2, 8, 9]. Initially, the rock bolt provides very stiff resistance to shear deformation. With increasing shear deformation, two plastic hinges form symmetrical to the discontinuity. The length between these two plastic hinges is called the active length. The local reinforcement model in 3DEC assumes that only this active length provides shear and axial resistance to shear deformation.

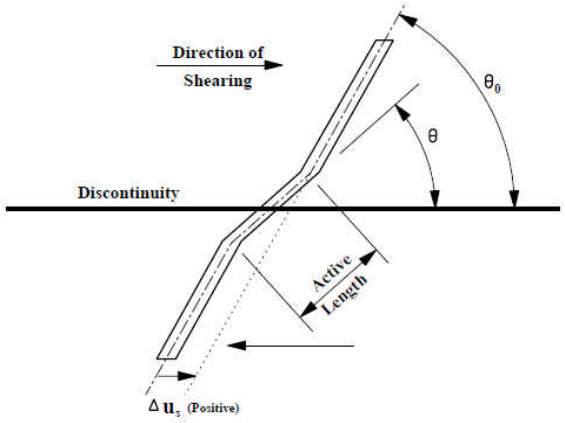

Fig. 3. Reinforcement geometry after shear displacement [10, 19].

The local reinforcement model in 3DEC is a simple and very effective way of modeling the local effect of reinforcement where it passes through the discontinuity. This methodology is very suitable in hard rock when deformation of individual blocks may be neglected in comparison with deformation of the reinforcement system. However, modeling the local effect of the reinforcement near a discontinuity may not be sufficient to model correct load transfer of the reinforcement in the weaker rocks found in a coal mine. FLAC3D pile structural elements (or UDEC rockbolt structural elements) therefore seem more suitable for coal mining applications. However, pile structural elements should also show the realistic local effect that is shown by the local reinforcement model implemented in 3DEC.

4. THE PERFORMANCE OF THE FLAC3D ROCK BOLT MODEL FOR HARD ROCK

In order to evaluate the performance of the FLAC3D pile element (Rock Bolt Element) for hard rocks, illustrative examples used by Lorig [10] to evaluate the performance of the local reinforcement model in UDEC were simulated with FLAC3D. By using the pile elements, the shear force and stiffness of the bolt can be simulated by the combined behavior of the bending resistance of the pile element and normal coupling spring resistance. In the axial direction, the elastic modulus and strength of the pile element and shear resistance and stiffness of shear coupling spring simulate axial behavior.

4.1. The Performance of the UDEC/3DEC Local Reinforcement Model for Hard Rock

Using the local reinforcement method in UDEC, Lorig [10] duplicated the results of the shear tests [1] on natural fractures and machined surfaces, with a normal pressure of 0.17 MPa and reinforcement perpendicular to the discontinuity. Figure 4 shows the test results published by Haas [1]. For the numerical simulation of the test on a machined surface, Lorig assumed a non-dilatant discontinuity friction angle of 50°. For the natural fractural surface, he assumed the peak friction angle as 65.5° and the residual friction angle as 50°. He also indicated that the interface friction angle reduced to the residual value in 13 mm of displacement. The initial dilatation angle was 15.6° and this angle reduced to a residual of 0° in 13 mm. Table 1 shows the test parameters used by Haas [1] and Lorig [10].

Table.1 Test parameters for UDEC local reinforcement model [10].

Limestone Properties				
UCS (MPa)	*Elastic Modulus (GPa)*	*Poisson's Ratio*		
6.3	33.8	0.18		
Resin Grout Properties				
Unconfined Compressive Strength (MPa)	*Shear Modulus (GPa)*			
110	3.7			
Reinforcement (Bolt) Properties				
Yield Strength (MPa)	*Ultimate Strength (MPa)*	*Elastic Modulus (GPa)*	*Bolt Diameter (mm)*	*Hole Diameter (mm)*
275	520	200	22	35

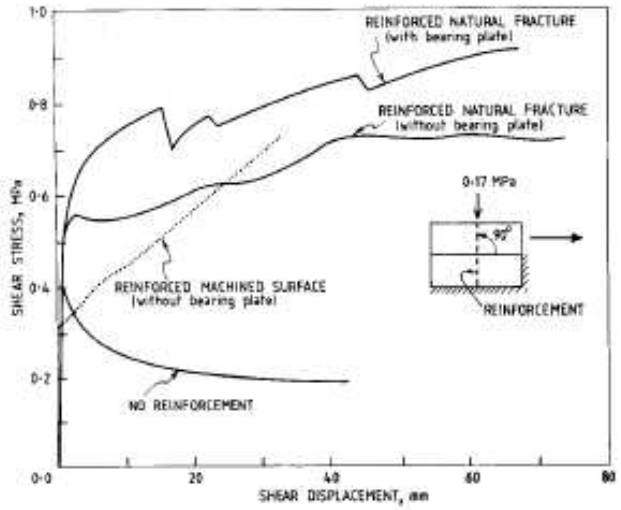

Fig. 4. Test results published by Haas [1].

Lorig [10] used the local reinforcement method to model a series of tests performed on smooth rock surfaces with bolts oriented at 45°, 90°, and 135° to the discontinuity surfaces. Results of the numerical model [10] are shown in Figure 5. The numerical simulation results with UDEC show reasonable agreement with the laboratory data published by Haas [1].

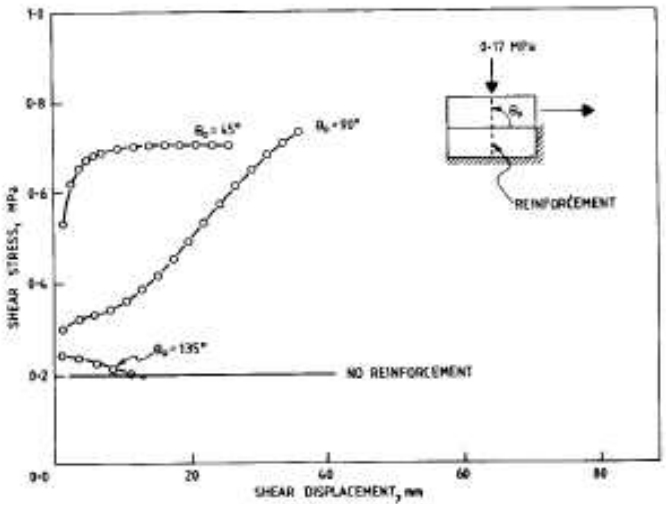

Fig. 5. Local reinforcement model results of Lorig [10].

4.2. FLAC3D Model Results

The same tests were simulated with the FLAC3D rock bolt model. The interface friction angle and normal pressure were set to the same values used by Lorig [10]. The actual bolt lengths used during the tests [1] were used in the model. Lorig [10] indicated that Haas [1] did not include the complete force-displacement response from the pull tests, but he reported an axial stiffness of 550 MN/m and an ultimate capacity of 140 kN for the reinforced system. In order to get similar axial behavior with FLAC3D, a pull test model was developed and the shear coupling spring stiffness and cohesion were adjusted to result in a similar axial stiffness and ultimate capacity as reported by Haas [1]. The normal coupling

spring stiffness and cohesion were also calibrated to match the test results. Table 2 shows the calibrated FLAC3D input parameters. Figure 6 shows the results of the calibrated model.

Table 2. Calibrated FLAC3D model parameters.

Spring Stiffness (MN/m)		**Spring Cohesion (MPa)**		**Plastic Moment (kN-m)**	**Segment Size (mm)**
Normal Spring	*Shear Spring*	*Normal Spring*	*Shear Spring*		
25	*0.065*	*0.3*	*1.5*	*1.5*	*5*

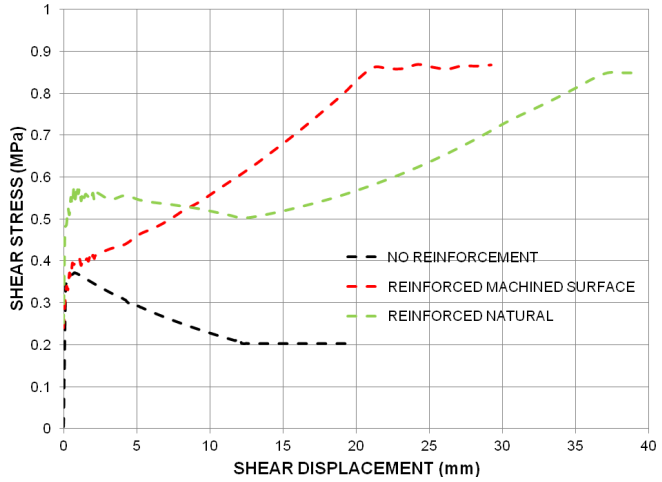

Fig. 6. FLAC3D model results of the Haas [1] tests of bolts that are perpendicular to the discontinuity surface.

Numerical models with FLAC3D were run to simulate the UDEC test results with bolts oriented at 45°, 90°, and 135° to the discontinuity surfaces as shown in Figure 5. Figure 7 shows the FLAC3D results. In the FLAC3D pile structural element model, the pile elements cannot fail in compression. In order to simulate compressive yielding in the 135° inclined bolts, the plastic moment limit was set to a smaller value (1.0 kN-m) in the current study model, which allowed the bolt to yield with a compressive strength equal to the magnitude of the tensile yield strength (Table 2). When the bolt was oriented 45° to the discontinuity surface, tensile force mobilized in the bolt very quickly compared to shear forces (and moment), and the system ultimately yielded due to excess tensile stress. Maximum moment on the bolt was below the plastic moment limit (Table 2). When the bolt was oriented at 135°, compressive forces mobilized quickly on the bolt, and similarly to the 45° orientation, the maximum moment on the bolt was below the plastic moment limit (Table 2). The FLAC3D model results (Figure 7) showed reasonable agreement with the experimental study and UDEC local reinforcement model results (Figure 5).

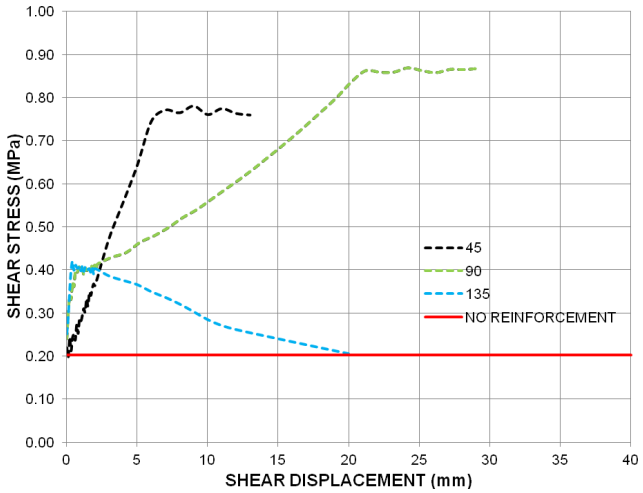

Fig. 7. FLAC3D model results (bolt oriented 45°, 90° and 135°)

Lorig [10] assumed the active length of the local reinforcement to be 90 mm. Figure 8 shows the moment distribution on the bolt calculated by FLAC3D. According to Figure 8, the active length is 88 mm. Active length was calculated by measuring the distance between the two plastic hinge locations on the bolt, and the plastic hinge locations were determined based on the location of the maximum moment in the bolt. The active length that was assumed by Lorig [10] and calculated from FLAC3D results are close to each other.

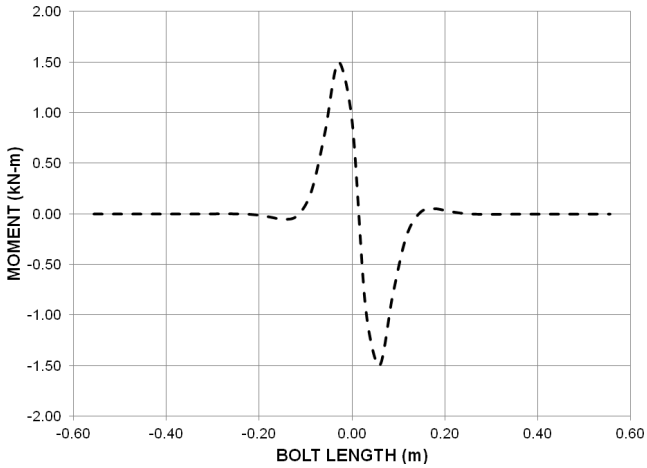

Fig. 8. Moment distribution in the bolt and plastic hinge locations calculated by FLAC3D.

The FLAC3D model results show the expected theoretical and observed test behaviors. Maximum shear stress seen on the discontinuity and shear stresses are zero at the maximum moment locations (at the plastic hinge locations) (Figure 9). Stress and moment decays into the rock within 150-180 mm from the joint (Figure 8, Figure 9). Therefore, it appears that adequate representation of bolt shear resistance and load transfer can be achieved by properly calibrating the FLAC3D pile structural element model.

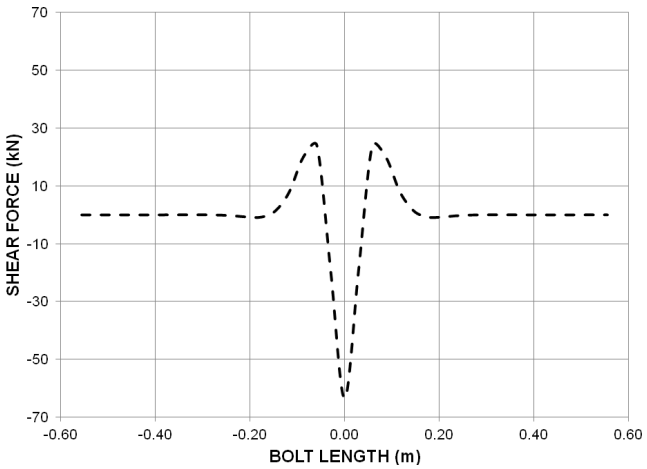

Fig. 9. Shear force distribution in the bolt

5. CALIBRATION OF THE FLAC3D ROOF BOLT MODEL WITH TEST RESULTS

McHugh and Signer [2] indicated that shear loading contributes significantly to the failure of rock bolts used in coal mines. They performed 17 laboratory direct shear tests on rock joints that were reinforced by fully grouted rock bolts. Each bolt was instrumented with a total of 14 strain gages at 7 different locations to investigate the axial and bending stress distribution on the bolt. The test setup is shown in Figure 10.

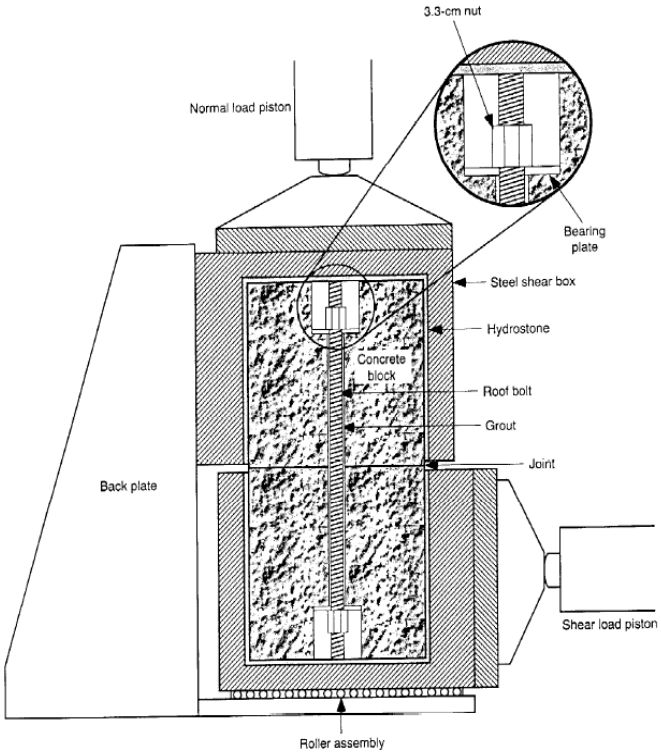

Fig. 10. Direct shear test setup of reinforced joint [2].

5.1. FLAC3D Model Generation

Test results published by McHugh and Signer [2] were used to calibrate FLAC3D model of the reinforced joint shear test. The test parameters [2] used to generate the FLAC3D model geometry (Figure 11) are shown in Table 3. Similar to the test setup, two 29-cm cubical blocks with an interface between them were generated. FLAC3D zones were gridded to have 2.9-cm cubical zones. Interface normal and shear stiffness were calculated based on the recommendation of Itasca [20]. A 58-cm-long bolt perpendicular to the interface was generated with 5-mm-long pile structural elements.

Table 3. Test parameters for FLAC3D bolt shear test [2].

Bolt length (cm)	58.4
Bolt diameter (mm)	22
Concrete block size (cm)	29 (w) x 29 (l) x 29 (h)
Hole diameter (mm)	28.6
Resin UCS (MPa)	69
Concrete UCS (MPa)	85.5
Concrete elastic modulus (GPa)	33.8
Concrete Poisson's Ratio	0.18
Bolt yield load (kN)	160
Bolt ultimate load (kN)	233
Normal force on the interface (kN)	8.9
FLAC3D Zone Size (cm)	2.9

After the generation of the model geometry, boundary conditions of the model were set to represent the same loading and deformation characteristics of the test setup (Figure 10). Displacement boundary conditions were applied to the model. The upper block was fixed in the vertical (Z axis) and horizontal (X axis) directions. A normal force of 8.9 kN was applied to the bottom of the lower block (Figure 11). The model was run to achieve its equilibrium state with the normal force on the lower block. Then a constant horizontal velocity in the negative "X" direction was applied to the right side of the lower block. The total shear force applied to the model was calculated from the grid point reactions. Also, interface normal and shear forces were calculated from the interface nodes and monitored during each time step. During the model run, shear force, tensile force, moment on the bolt elements, and failure state of the normal spring were also monitored.

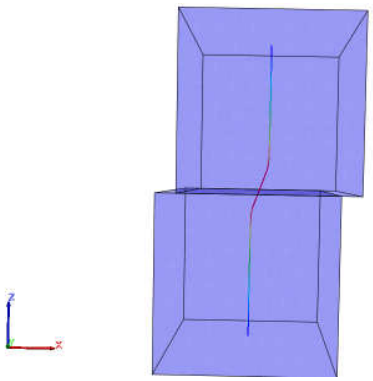

Fig. 11. FLAC3D model geometry.

The only difference between the laboratory tests and the FLAC3D model was the pretension. McHugh and Signer [2] applied different pretension values to the rock bolts, but they observed that pretension did not affect the yield and ultimate applied shear force. Other researchers also indicated similar results [1], but it is also known that pretension can increase the initial stiffness of the system [9].

5.2. Pile Structural Element Failure Criterions

There are two possible failure mechanisms of the bolt during the shear loading: 1) Yielding of the bolt starts with the formation of the hinge points within a 1-5 mm shear displacement along the joint. Beyond the yield limit, the bolt deforms plastically and fails under the action of shear and tensile forces [2, 8, 9]; or, 2) if the surrounding rock is very stiff and hard, the bolt can fail directly due to shear (direct shear failure) without any plastic hinge formation [7, 14].

FLAC3D pile structural elements can only yield in the axial direction. In this paper, the plastic moment limit (Table 4) was set to simulate the formation of the plastic hinges at the locations of the maximum moment in the bolt. When the plastic moment limit is reached, the shear force on the bolt stays constant, but the axial force continues to increase between the two plastic hinges. In the FLAC3D pile structural element model, elastic perfectly plastic behavior was assumed, but it is also possible to simulate the tensile rupture of the bolt by adding a maximum tensile failure strain to the model input. Therefore, the effect of shear forces on failure and direct shear failure cannot be simulated by using the original yield/failure criterion of the FLAC3D pile elements.

In this paper, a second type of yield/failure criterion (different from the original FLAC3D pile element yield/failure criterion) was artificially implemented by using the FISH option of FLAC3D. In this updated yield/failure criterion, the initial yielding of the bolt is determined by using Eq. 1 and the ultimate failure of the bolt is determined by using Eq. 2.

In order to determine the yield condition, Eq. 1 is calculated. "T_{ty}" (axial yield load) and "M_{pl}" (plastic moment) are input parameters for the FLAC3D pile element model. "T_{tx}" (axial load on the pile element) and "M_z" (moment on the pile element) are monitored in each "FLAC3D time step." These values are assigned to the FISH variables and Eq. 1 is calculated inside the FISH function. If the calculated value of Eq. 1 is less than "1," the bolt is in the elastic range. If the calculated value is equal to or greater than "1," the plastic moment limit of the pile element is changed to the value of "M_z" and the pile element is forced into bending yield immediately.

In order to determine the failure condition, Eq. 2 is calculated. "T_{tu}" (ultimate axial load) and "V_u" (ultimate shear load) are bolt properties and they are assigned to FISH variables. "T_{tx}" (axial load on the pile element) and "V" (shear load on the pile element) are monitored in each "FLAC3D time step." These values are assigned to the FISH variables and Eq. 2 is calculated inside the FISH function. If the calculated value is equal to or greater than "1," the axial yield load limit of the pile element is changed to the value of "T_{tx}" and the pile element is forced into tensile yield.

By using this updated yield/failure criterion, the effect of shear forces, bending, and direct shear failure can be simulated. Figure 12 shows the simulation of possible failure mechanisms with updated yield/failure criterion.

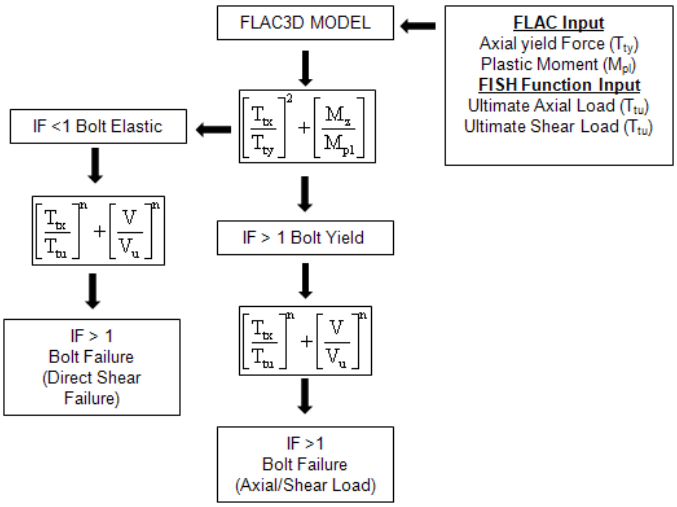

Fig. 12. Failure mechanics with updated criterion.

5.3. FLAC3D Model Results

Figure 13 shows the results of the calibrated model with bending and shear failure compared to the laboratory test results. The average line (red line) shown in Figure 13 is drawn through the average of the test data. The "FLAC3D original yield/failure" line (black dotted line) shows the shear resistance of the reinforced joint calculated by using the default pile element yield/failure criterion implemented in FLAC3D. The "FLAC3D updated yield/failure" line (green dotted line) shows the shear resistance of the reinforced joint calculated by using yield/failure criterion detailed in Figure 12. The system behavior for both criteria is very similar.

This system behavior can be divided into three different stages. In the first stage, the shear load increases with a small displacement (5 mm). In this stage, the stiffness of the system depends on the rotational stiffness of the structural elements and the normal coupling spring stiffness. With increasing shear deformation, the slope of the curve changes as the grout/rock fails due to crushing and the structural element yields in bending due to excess moment. This transition point is determined by the plastic moment limit and normal coupling spring

cohesion. In the original yield/failure criterion, the plastic moment is equal to the FLAC3D input value (Table 4). For the updated yield/failure criterion, the plastic moment was calculated from Eq. 1. For this bolt orientation (90° to the discontinuity), the maximum mobilized tensile force in the pile elements is less than 1% of the yield load of the bolt during the initial 1-5 mm shear deformation of the discontinuity. However, the mobilized moment in the pile element was more than the 99% of the plastic moment limit (almost equal to the plastic moment limit in Table 4). Therefore, both criteria calculated essentially the same yield point (Figure 13).

After this bending stage, the system behavior is controlled by the bolt elastic modulus, shear coupling spring stiffness, cohesion, and the bolt tensile yield strength. The maximum shear force in the bolt stays constant after the yield point. In the FLAC3D model, the maximum shear force at the failure point was equal to 42% of the ultimate axial load (233 kN), where the ultimate shear load of the bolt was assumed to be 50% of the ultimate axial load [6]. In the original yield criterion, the ultimate failure point was reached when the maximum tensile force on the pile element was equal to the bolt yield force (160 kN). For the updated failure criterion, the required tensile failure load was calculated from Eq. 2. In this model "n=2" for Eq. 2 was found suitable [14], and axial failure load was calculated as 121 kN (52% of the ultimate axial load). Figure 13 shows that the updated yield/failure criterion gave better estimation of the ultimate failure load for the test results published by McHugh and Signer [2].

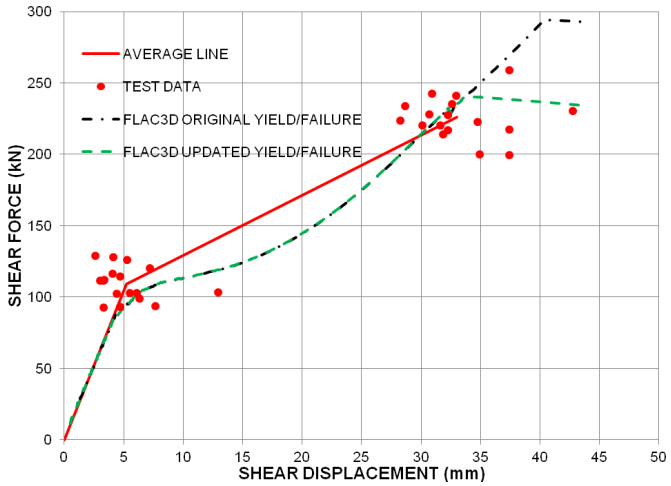

Fig. 13. Comparison of the calibrated FLAC3D model with actual data.

The calibrated parameters of the model are shown in Table 4. These parameters were calibrated based on the direct shear test results shown in Figure 13. The plastic moment and normal cohesion limits were set to match the yield point shown in Figure 13. At the yield point, the system shear displacement is around 5 mm and the shear force is between 100 and 150 kN. The stiffness of the normal spring is set to match the initial stiffness of the system. The shear spring stiffness and cohesion are set to match the system behavior between the yield point and ultimate point. It is recommended to calibrate the shear coupling spring parameters based on a pull test (if available) and the normal spring parameters and plastic moment based on a direct shear test.

Table.4 Calibrated parameters of the model.

Spring Stiffness (MN/m)		**Spring Cohesion (MPa)**		**Plastic Moment (kN-m)**	**Segment Size (mm)**
Normal Spring	***Shear Spring***	***Normal Spring***	***Shear Spring***		
1.0	*0.2*	*2.75*	*0.8*	*2.0*	*5*

Figure 14 shows the contribution from each individual component (total shear resistance, bolt shear resistance, etc.) to the total bolt shear resistance [8]. The individual loads were normalized by dividing the load contribution of the individual loading component by the ultimate load carrying capacity of the bolt (Table 3). Initially, the bolt shear resistance (the dowel effect) provided the most resistance to shear movement (the red line [original Y/F] and blue line [updated Y/F] in Figure 13). Then, after the formation of the plastic hinges (after 5-10 mm of shear displacement) similar to the analysis of Holmberg and Stille [14], Pellet and Egger [15], and Ferrero [13], the shear resistance of the bolt was constant. At this point, the tensile resistance in the direction of shear started to mobilize. The frictional resistance along the interface was constant between 0 and 10 mm of shear displacement and this was due to the initial normal force applied on the interface (Table 3) and the interface friction angle. After 10 mm of shear displacement, additional frictional force was mobilized along the interface due to the normal component of the mobilized tensile resistance of the bolt.

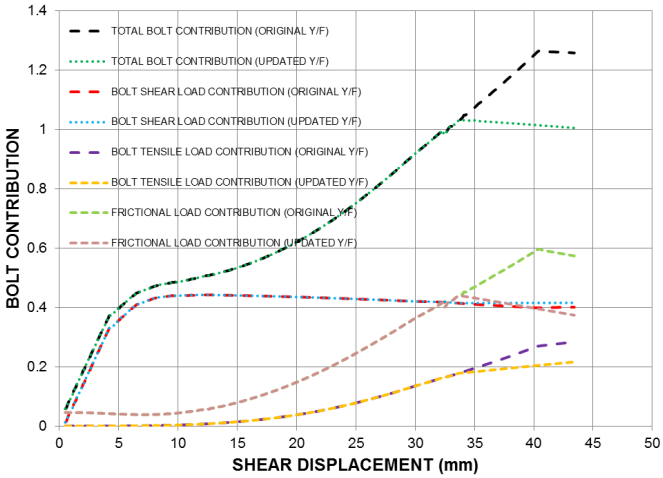

Fig. 14. The contribution of different load components on total bolt load.

5.4. *The Effect of Pile Element Size and Normal Spring Stiffness on Model Results with the Original Yield/Failure Criterion*

The bolt segment size was initially selected as 5 mm in the calibrated model to simulate the maximum moment locations (plastic hinge locations) as accurately as possible. In order to investigate the effect of the segment size on the model results, the segment size was varied up to 60 mm and the results analyzed.

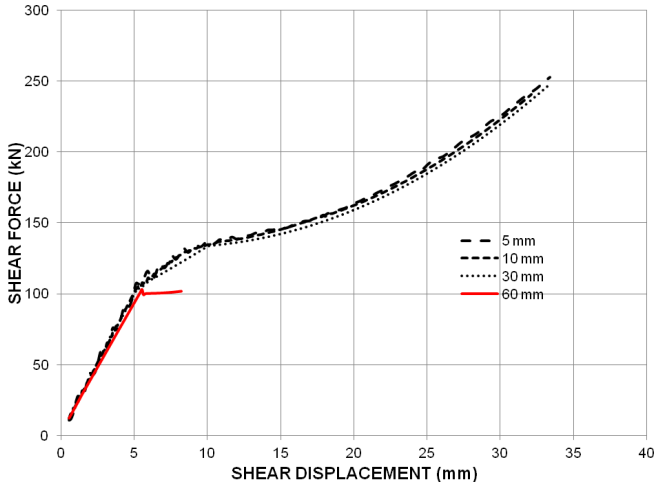

Fig. 15. Effect of bolt segment size on system behavior.

Figure 15 shows the results of this parametric study. When the segment size is less than the half of the active length (active length is 88 mm), there is not any significant change on the system behavior; however the larger segment sizes greatly change the behavior. When the larger segments are used, there is rotational stiffness of the structural elements hence the initial system stiffness decreases. The distance between the two maximum moment locations adjacent to the interface increases and the magnitudes of the moment and shear force mobilized in the bolt decrease. In addition, the stiffness of the system behavior between the yield load and ultimate load location decreases.

In the FLAC3D rock bolt model, crushing and deformation of the rock and grout are essentially simulated by the coupling springs. In order to simulate the effect of the rock strength and stiffness, normal spring stiffness is adjusted. Figure 16 shows the effect of normal spring stiffness on the system behavior. Initial stiffness of the system increased with the increasing normal spring stiffness. When the normal spring stiffness is increased, the spring's reaction to deformation of the discontinuity also increases. Normal forces on the springs increase more rapidly with any shear deformation. This rapid increase of the normal spring forces causes faster mobilization of the shear forces and moments on the pile elements as observed in the higher normal spring stiffness curves in Figure 16.

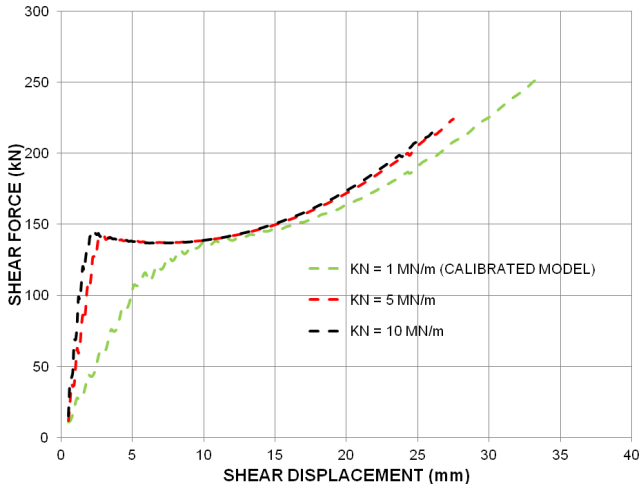

Fig. 16. Effect of normal stiffness on system behavior.

5.5. *Simulation of Direct Shear Failure of the Bolt with Updated Yield/Failure Criterion*

In order to simulate the direct shear failure of the bolt, the calibrated model normal coupling spring stiffness was greatly increased to 20 MN/m, cohesion was increased to 3.75 MPa, and plastic moment limit was increased to 2.5 KN-m. Figure 17 shows the change of the shear force/displacement graph of the reinforced joint model with the updated yield/failure criterion. Figure 17 shows that the bolt now fails between 1 and 1.5 mm of shear deformation of the discontinuity. Figure 18 shows the moment in the bolt during this test. The maximum moment in the bolt is less than the plastic moment value set in this model (2.5 kN-m). However, the shear force in the bolt is more than the ultimate shear force (50% of the ultimate axial force = 1.165 kN). Therefore, in this particular model, the shear force in the bolt mobilized much faster than the moment (Figure 19). As shown in Figure 12, the bolt reached its ultimate shear load before reaching its moment yielding limit (based on Eq. 1). Holmberg and Stille [14] also indicated that this type of direct shear failure is possible.

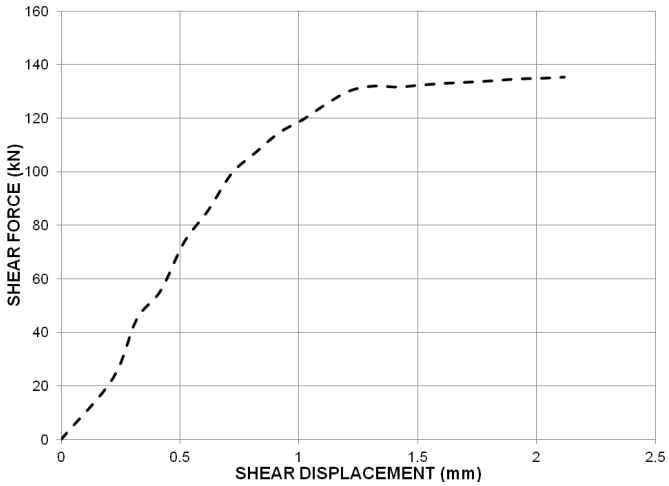

Fig. 17. Shear force vs. shear deformation during the direct shear failure of the bolt.

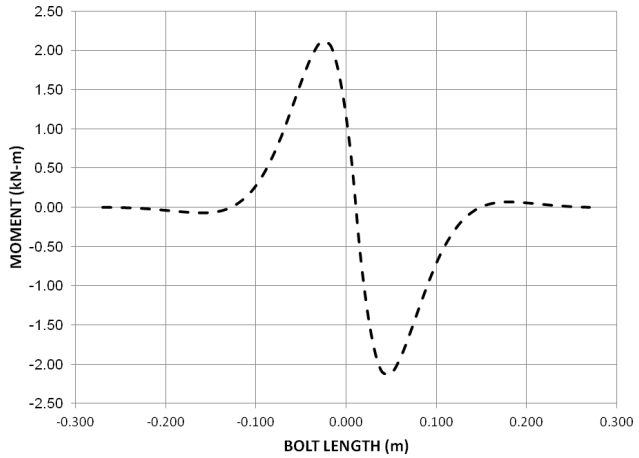

Fig. 18. Moment in the bolt during the direct shear failure of the bolt.

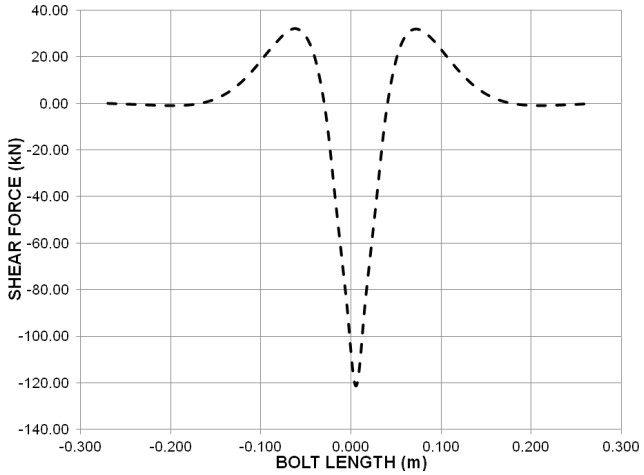

Fig. 19. Shear force in the bolt during direct shear failure of the bolt.

6. CONCLUSIONS

In this paper, results of the shear tests of reinforced rock joints published by Haas [1] and McHugh and Signer [2] were modeled with FLAC3D to identify and calibrate the critical parameters of the rock bolt model both in tension and in shear. It was observed from the model results that the modeled roof bolt provides resistance to horizontal movement by the following mechanisms:

1) The bending stiffness and grout/rock resistance (dowel effect) causes direct shear resistance to the shear movement of the joint (Figure 14).
2) After the initiation of the shear deformation, the elongation of the bolt causes tensile resistance, and the normal component of the tensile resistance causes an increase in normal stress on the joint plane which thereby causes increased frictional resistance (Figure 14). With a dilating joint, dilation of the interface can increase the mobilization rate of the tensile force of the bolt and enhance the mechanical interlock between joint surfaces (Figure 6).
3) The horizontal component of the mobilized tensile force in the bolt creates direct resistance to the shear movement (Figure 14).

Experimental studies and theoretical analysis show that the failure mechanisms of roof bolts depend on the surrounding host rock characteristics. Failure of the bolt when surrounded by hard and stiff rock is likely to be due to direct shear or a combination of shear and tension. Failure of the bolt when surrounded by weak rock is more likely to be due to tensile strength or ultimate elongation. This investigation indicates that there are two possible failure mechanisms of bolts during shear loading at a joint, as described below.

In softer rock during failure, yielding of the bolt starts by the formation of plastic hinges on the bolt due to the combined effect of bending and axial loads. Beyond the yield limit, the bolt behaves plastically until it reaches its ultimate plastic limit and ruptures under the action of the axial and shear forces. In the FLAC3D model with its original yield/failure criterion, this bending failure mechanism was modeled with the pile elements (rock bolt) (Figure 13). In order to obtain correct load transfer and loading behavior in the model, it was found that the size of the structural elements should not be larger than the half of the active length of the bolt (Figure 15). Shear spring stiffness and cohesion should be calibrated based on pull test results and normal spring stiffness and cohesion should be calibrated based on shear test results.

The calibrated model gave similar load/deformation and failure responses observed during the tests [17]. Initially, shear force and moment of the structural elements 150-180 mm from the joint increased rapidly with shear displacement of the joint (< 5 mm). Maximum shear force on the bolt mobilized at the interface and increased until the maximum moment on the bolts reached the plastic moment limit. When the plastic moment limit was reached, plastic hinges formed. After that, maximum shear force on the bolt was constant (Figure 14) and tensile force started to mobilize between the plastic hinges (Figure 11). Tensile force on the bolt continued to increase until it reached the tensile yield strength of the bolt.

If the surrounding rock is very stiff and hard, the bolt can fail directly due to shear (direct shear failure) without any formation of plastic hinges [7, 14]. It was found that original yield/failure criterion of the pile elements in FLAC3D cannot model this behavior directly. In order to model the direct shear failure of the bolt and include the effect of shear forces on the first type of failure, an updated yield/failure criterion was implemented with the FISH option of FLAC (Figure 12). Model results showed that by using this simple FISH algorithm, the direct shear failure of the bolt surrounded by a stiff hard rock can be simulated (Figure 17).

In conclusion, it was found that a good correspondence was established between the correctly calibrated FLAC3D roof bolt model and experimental results. This showed that the FLAC3D roof bolt model can simulate the lateral shearing of the bolts accurately. During the study, the effect of the shear loads in the bolt was incorporated into the model, and it was found that shear loads also play a very important role on the failure of the bolt. It was also shown that by updating the yield/failure criterion of the FLAC model, similar results with the complex analytical methods developed to model the grouted roof bolt performance can be simulated.

7. DISCLAIMER

The findings and conclusions in this paper are those of the authors and do not represent the views of the National Institute for Occupational Safety and Health (NIOSH). Mention of any company name, product, or software does not constitute endorsement by NIOSH.

REFERENCES

1. Haas C. J. 1976. Shear resistance of rock bolts. *Journal of Transactions, Society of Mining Engineers of AIME*. pp. 32–41.
2. McHugh E. and S. P. Signer. 1999. Roof bolt response to shear stress: laboratory analysis. In *Proceedings of the 18th International Conference on Ground Control in Mining*. Morgantown, WV. pp. 232–238.
3. Peng S. S. 2008. *Coal mine ground control*. 3rd ed. Morgantown, WV. pp. 147–222.
4. Serbousek M. O. and S. P. Signer. 1987. *Linear Load-Transfer Mechanics of Fully Grouted Roof Bolts*. RI-9135 USBM.
5. Li C. and B. Stillborg. 1999. Analytical models for rock bolts. *Int J Rock Mech Min Sci.* 36:1013–29.
6. Firth, R. C. and M. Colwell. 2011. Why Dead Load Suspension Design For Roadway Roof Support is Fundamentally Flawed Within a Pro-Active Strata Management System. In *Proceedings of the 30th International Conference on Ground Control in Mining.* pp. 118–125.
7. Bjurström, S. 1974. Shear strength of hard rock joints reinforced by grouted untensioned bolts. *Proceedings of the 3rd ISRM Congress, Denver, USA*, pp. 1194–9.
8. Grasselli, G. 2005. 3D Behavior of bolted rock joints: experimental and numerical study. *Int. J. Rock Mech. Min Sci.* 42: 13–24.
9. Jalalifar, H. and N. Aziz. 2010. Experimental and 3D Numerical Simulation of Reinforced Shear Joints. *Rock Mech Rock Eng.* 43:95–103.
10. Lorig, L. J. 1985. A Simple Numerical Representation of Fully Bonded Passive Rock Reinforcement for Hard Rocks. *Computer and Geotechnics.* 1: 79–97.
11. Fairhurst, C. and B. Singh. 1974. Roof Bolting in Horizontally Laminated Rock *Eng And Min J, Feb*, pp. 80–90.
12. Gerdeen, J. C., V. W. Snyder, G. L. Viegelahn and J. Parker. 1977. *Design criteria for roof bolting plans using fully resin-grouted nontensioned bolts to reinforce bedded mine roof.* U.S. Bureau of Mines OFR 46 (4)–80.
13. Ferrero, A. M. 1995. The shear strength of reinforced rock joints. *International Journal of Rock Mech. Min. Sci. Geomech. Abst*, 32:595–605.
14. Holmberg, M. and H. Stille. 1992. The mechanical behavior of a single grouted bolt. *International Symposium on Rock Support in Mining and Underground Construction, Sudbury, Canada*. pp. 73–81.
15. Pellet, F. and P. Egger. 1996. Analytical model for the mechanical behavior of bolted rock joints subjected to shearing. *Rock Mech Rock Eng.* 29:73–97.
16. Haas C. J. 1981. Analysis of rock bolting to prevent shear movement in fractured ground. *Min. Eng*. 33:698–704.
17. Itasca Consulting Group, Inc. 2009. *FLAC3D – Fast Lagrangian Analysis of Continua, in 3 Dimensions, Structural Elements.* 4th ed., Minneapolis, MN.
18. Brady, B. H. G. and E. T. Brown. 2004. *Rock Mechanics for underground mining*. 4th ed. Dordrecht: Kluwer Academic Publishers.
19. Itasca Consulting Group, Inc. 2009. *3DEC – Three Dimensional Distinct Element Code, Structural Elements.* 4th ed., Minneapolis, MN.
20. Itasca Consulting Group, Inc. 2009. *FLAC3D – Fast Lagrangian Analysis of Continua, in 3 Dimensions, Theory and Background.* 4th ed., Minneapolis, MN.